ELECTRICAL, STRUCTURAL, AND OPTICAL PROPERTIES OF CR-DOPED AND NON-STOICHIOMETRIC V_2O_3 THIN FILMS (POSTPRINT)

Patricia A. Metcalf, Shekhar Guha, Leonel P. Gonzalez, Jacob O. Barnes, Elliott B. Slamovich, and Jurgen M. Honig

Hardened Materials Branch
Survivability and Sensor Materials Division

JUNE 2006

AIR FORCE RESEARCH LABORATORY
MATERIALS AND MANUFACTURING DIRECTORATE
WRIGHT-PATTERSON AIR FORCE BASE, OH 45433-7750
AIR FORCE MATERIEL COMMAND
UNITED STATES AIR FORCE

NOTICE AND SIGNATURE PAGE

*//Signature//   //Signature//

SHEKHAR GUHA, Ph.D.   MARK S. FORTE, Acting Chief
Agile IR Limiters   Hardened Materials Branch
Exploratory Development   Survivability and Sensor Materials Division
Hardened Materials Branch

//Signature//

TIM J. SCHUMACHER, Chief
Survivability and Sensor Materials Division

REPORT DOCUMENTATION PAGE

*Form Approved
OMB No. 0704-0188*

The public reporting burden for this collection of information is estimated to average 1 hour per response, including the time for reviewing instructions, searching existing data sources, searching existing data sources, gathering and maintaining the data needed, and completing and reviewing the collection of information. Send comments regarding this burden estimate or any other aspect of this collection of information, including suggestions for reducing this burden, to Department of Defense, Washington Headquarters Services, Directorate for Information Operations and Reports (0704-0188), 1215 Jefferson Davis Highway, Suite 1204, Arlington, VA 22202-4302. Respondents should be aware that notwithstanding any other provision of law, no person shall be subject to any penalty for failing to comply with a collection of information if it does not display a currently valid OMB control number. **PLEASE DO NOT RETURN YOUR FORM TO THE ABOVE ADDRESS**.

1. REPORT DATE *(DD-MM-YY)*	2. REPORT TYPE	3. DATES COVERED *(From - To)*
June 2006	Journal Article Postprint	

4. TITLE AND SUBTITLE
ELECTRICAL, STRUCTURAL, AND OPTICAL PROPERTIES OF CR-DOPED AND NON-STOICHIOMETRIC V_2O_3 THIN FILMS (POSTPRINT)

5a. CONTRACT NUMBER
In-house

5b. GRANT NUMBER

5c. PROGRAM ELEMENT NUMBER
62102F

6. AUTHOR(S)
Patricia A. Metcalf, Elliott B. Slamovich, and Jurgen M. Honig (Purdue University)
Shekhar Guha (AFRL/MLPJ)
Leonel P. Gonzalez and Jacob O. Barnes (General Dynamics Information Technology, Inc.)

5d. PROJECT NUMBER
4348

5e. TASK NUMBER
RG

5f. WORK UNIT NUMBER
M08R1000

7. PERFORMING ORGANIZATION NAME(S) AND ADDRESS(ES)

Purdue University
West Lafayette, IN

Hardened Materials Branch (AFRL/MLPJ)
Survivability and Sensor Materials Division
Materials and Manufacturing Directorate
Wright-Patterson Air Force Base, OH 45433-7750
Air Force Materiel Command, United States Air Force

General Dynamics Information
 Technology, Inc. (formerly Anteon
 Corporation)
5100 Springfield Pike, Suite 509
Dayton, OH 45431-1264

8. PERFORMING ORGANIZATION REPORT NUMBER
AFRL-ML-WP-TP-2007-560

9. SPONSORING/MONITORING AGENCY NAME(S) AND ADDRESS(ES)
Air Force Research Laboratory
Materials and Manufacturing Directorate
Wright-Patterson Air Force Base, OH 45433-7750
Air Force Materiel Command
United States Air Force

10. SPONSORING/MONITORING AGENCY ACRONYM(S)
AFRL/MLPJ

11. SPONSORING/MONITORING AGENCY REPORT NUMBER(S)
AFRL-ML-WP-TP-2007-560

12. DISTRIBUTION/AVAILABILITY STATEMENT
Approved for public release; distribution unlimited.

13. SUPPLEMENTARY NOTES
Journal article published in Thin Solid Films, Vol. 515, 2007.

© 2006 Elsevier B.V. The U.S. Government is joint author of this work and has the right to use, modify, reproduce, release, perform, display, or disclose the work. PAO Case Number: AFRL/WS 06-1716, 11 Jul 2006.

14. ABSTRACT
V_2O_3 films and Cr-doped V_2O_3 films were grown on (0 0 0 1) (C-plane) and (1 1 2 0) (A-plane) oriented sapphire substrates by the reduction of sol-gel derived vanadium oxide films. Examination by X-ray diffraction, scanning electron microscopy, transmission electron microscopy, and atomic force microscopy showed the films to be comprised of highly oriented grains. Optical transmission and resistivity measurements revealed phase transitions characteristic of the single crystal V_2O_3 and Cr-doped V_2O_3. Subsequent anneals of the un-doped films under controlled oxygen atmospheres yielded non-stoichiometric films with metal-insulator transitions characteristic of annealed V_2O_3 single crystals.

15. SUBJECT TERMS
Phase Transitions, Vanadium Oxide, Optical Properties, Electrical Properties

16. SECURITY CLASSIFICATION OF:			17. LIMITATION OF ABSTRACT:	18. NUMBER OF PAGES	19a. NAME OF RESPONSIBLE PERSON (Monitor)
a. REPORT Unclassified	**b. ABSTRACT** Unclassified	**c. THIS PAGE** Unclassified	SAR	12	Shekhar Guha
					19b. TELEPHONE NUMBER *(Include Area Code)* N/A

Standard Form 298 (Rev. 8-98)
Prescribed by ANSI Std. Z39-18

i

Electrical, structural, and optical properties of Cr-doped and non-stoichiometric V_2O_3 thin films

Patricia A. Metcalf [a,*], Shekhar Guha [c], Leonel P. Gonzalez [b], Jacob O. Barnes [b], Elliott B. Slamovich [a], Jurgen M. Honig [d]

[a] Materials Engineering, Purdue University, West Lafayette, Indiana, USA
[b] Materials and Manufacturing Directorate, Anteon Corp., Dayton, Ohio, USA
[c] Materials and Manufacturing Directorate, Air Force Research Laboratory, Wright Patterson AFB, Ohio, USA
[d] Department of Chemistry, Purdue University, West Lafayette, Indiana, USA

Abstract

V_2O_3 films and Cr-doped V_2O_3 films were grown on (0 0 0 1) (C-plane) and (1 1 $\bar{2}$ 0) (A-plane) oriented sapphire substrates by the reduction of sol–gel derived vanadium oxide films. Examination by X-ray diffraction, scanning electron microscopy, transmission electron microscopy, and atomic force microscopy showed the films to be comprised of highly oriented grains. Optical transmission and resistivity measurements revealed phase transitions characteristic of the single crystal V_2O_3 and Cr-doped V_2O_3. Subsequent anneals of the un-doped films under controlled oxygen atmospheres yielded non-stoichiometric films with metal-insulator transitions characteristic of annealed V_2O_3 single crystals.
© 2006 Elsevier B.V. All rights reserved.

Keywords: Phase transitions; Vanadium oxide; Optical properties; Electrical properties

1. Introduction

A variety of crystal phases exist in the vanadium–oxygen system, a number of which display dramatic changes in electronic, magnetic, and optical properties associated with phase transitions. Among the most interesting and widely studied is vanadium sesquioxide, V_2O_3, which upon cooling from room temperature exhibits a paramagnetic metal (PM) to antiferromagnetic insulator (AFI) phase transition at about 150 K. The metal-insulator transition temperature in V_2O_3 is sensitive to applied pressure, vanadium to oxygen ratio, and dopant concentration with elements like Cr and Ti [1–7]. For single crystal $V_{2-y}O_3$, the metal-insulator transition temperature decreases with an increase in oxygen excess. In $(V_{1-x}Cr_x)_2O_3$, with chromium doping of $x < 0.018$, the PM to AFI insulator transition temperature increases slightly with increasing chro-

mium concentration. In addition, $(V_{1-x}Cr_x)_2O_3$ samples doped with chromium ($0.005 < x < 0.018$) exhibit a paramagnetic metal to paramagnetic insulator (PI) phase transition at higher temperature. The crystal structure of V_2O_3 is rhombohedral in the PM and PI phases and monoclinic in the AFI phase. The PM to AFI phase transition is accompanied by a cell volume change, causing crystals to fracture when thermally cycled [8]. A generalized phase diagram for V_2O_3 as a function of temperature and chromium dopant concentration, at 1 atm pressure, is shown in Fig. 1. The phase diagram was determined from measurements of single crystal $(V_{1-x}Cr_x)_2O_3$ samples and controlled atmosphere annealed $V_{2-2y}O_3$ samples [6,7]. Since a hysteresis effect is encountered in resistivity measurements across the phase transition in crystals, this phase diagram depicts the results of measurements taken upon sample cooling.

In the past ten years, there have been a number of reports on the growth of thin films [9–16] and ultra-thin films [17–27] of V_2O_3 by reactive sputtering, reactive evaporation, pulsed laser deposition, and the sol–gel technique. By contrast, there are only two reports on the growth of Cr-doped V_2O_3 thin films
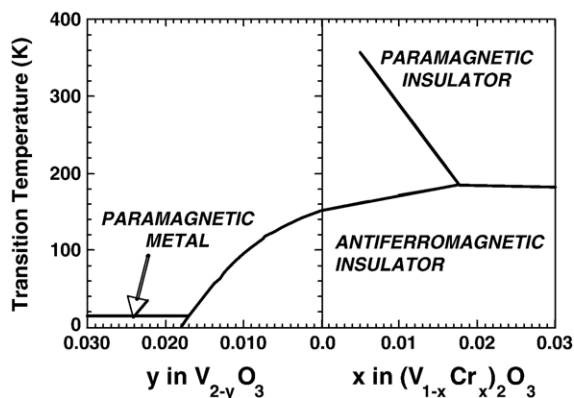

Fig. 1. Generalized phase diagram for the metal-insulator transition in single crystal $V_{2-y}O_3$ and $(V_{1-x}Cr_x)_2O_3$ as a function of temperature, data taken on cooling (extracted from Refs. [6,7]).

[28,29], and no reports on systematically prepared non-stoichiometric V_2O_3 thin films. Schuler et al. [12] reported that for V_2O_3 films grown epitaxially on (0 0 0 1) oriented sapphire substrates by reactive evaporation, the transition is broadened by the strain induced by lattice mismatch. It was proposed that the substrate–film interaction hinders the structural transition from the rhombohedral to monoclinic lattice. For ultra-thin films, less than 30 nm in thickness [23], the metal to insulator transition is completely suppressed by the substrate–film interaction.

Although a substantial amount of work has been done to study the effect on the electronic transition of doping single crystal V_2O_3 with chromium [1,6], little has been reported for chromium doped V_2O_3 films. Greenberg and Singleton [28] reported that for sol–gel derived chromium doped thin films, the conductivity "tended toward insulating" with increased chromium concentration. Based on resistivity measurements, Piao et al [29] reported an increase in the transition temperature with increasing chromium concentration, but attributed the absence of the higher temperature PM to PI transition to the small grain size in the sol–gel derived films.

2. Experimental details

V_2O_3 films were synthesized by heat-treating sol–gel derived vanadium oxide films in reducing atmospheres. The sol–gel films were prepared by spin-coating a solution of vanadium triisoprop-oxide, $VO(PrO)_3$, in isopropanol onto single crystalline, polished (0 0 0 1) (C-plane) and (1 1 $\bar{2}$ 0) (A-plane) oriented sapphire substrates. Sol–gel films were formed by the hydrolysis and condensation of neutral precursors in the ambient humidity. The films were dried at 85 °C, and the procedure was repeated to form one to nine layers. Chromium doped films were prepared by dissolving the chloride or acetylacetonate salts into isopropanol prior to the addition of the alkoxide. The amorphous, as-deposited films were then heat-treated in reducing atmospheres to obtain crystalline, 125 nm to 1250 nm thick V_2O_3 films. The vanadium oxide phases present in the annealed films depended on both the annealing atmosphere and temperature. V_2O_3 films were formed by heating the sol–gel films in a 5% hydrogen–95% argon gas

mixture at 850 °C for 2 h. The non-stoichiometric films were prepared by subsequent annealing of the V_2O_3 films in a vertical quench annealing furnace equipped with an oxygen sensor. The operational details of this system have been described elsewhere [30].

The resulting films were examined by X-ray diffraction (XRD), scanning electron microscopy (SEM), transmission electron microscopy (TEM), and atomic force microscopy (AFM). The XRD data were obtained using a Siemens DIFF500 diffractometer with Cu Kα radiation. JEOL 35CF, JEOL 2000FX, and Dimension 5000 microscopes were used to examine the microstructure of the films by SEM TEM, and AFM, respectively. The electrical resistance was measured using a standard four-probe technique. The optical transmission measurements were performed using a Perkin Elmer spectrum-GX Fourier transform infrared Spectrometer.

3. Results and discussion

3.1. X-ray diffraction and microscopy

The X-ray diffraction patterns of 300 nm thick V_2O_3 films deposited on (0 0 0 1) and (1 1 $\bar{2}$ 0) oriented sapphire substrates are presented in Fig. 2a and b. The results suggest that the films
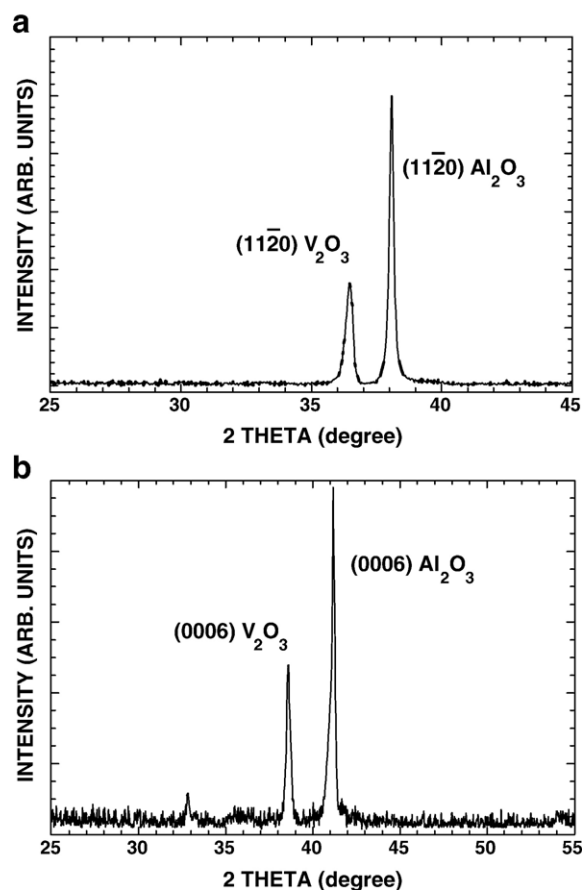

Fig. 2. XRD patterns of sol–gel derived vanadium oxide films. (a) The X-ray diffraction pattern of 300 nm thick V_2O_3 films deposited on (a) (1 1 $\bar{2}$ 0) oriented A-plane sapphire substrate and (b) (0 0 0 1) oriented C-plane sapphire substrate.

assume a preferred *c-axis* orientation on (0 0 0 1) oriented sapphire substrates and a preferred *a-axis* orientation on (1 1 $\bar{2}$ 0) oriented sapphire substrates. The X-ray diffraction patterns for films with thickness greater than 600 nm show the presence of other orientations, indicating a loss of preferred orientation in thicker films. In addition, it was found that preferred *a*-axis oriented V_2O_3 films could be grown on (0 0 0 1) oriented sapphire substrates by increasing the heating rates used to process the films.

Observation of the surface of a V_2O_3 film on sapphire by Scanning Electron Microscopy indicated that the film surfaces are relatively smooth. The TEM bright-field micrograph in Fig. 3 shows crystallites from a V_2O_3 thin film grown on C-sapphire at 925 °C. The sapphire substrate was ground from the reverse side of the film and remnants were transferred to a grid for examination by TEM. The V_2O_3 crystallites vary from 60 to 300 nm in diameter and are embedded in an amorphous matrix.

The surface morphology of a 300 nm thick V_2O_3 film on a (0 0 0 1) oriented sapphire substrate was examined using atomic force microscopy. The V_2O_3 film, which was grown by annealing for 2 h at 850 °C, was found to consist of grains oriented along the c-direction, consistent with the XRD results. The average grain size is about 60 nm, with a surface roughness of about 15 nm. An increase in temperature or annealing time resulted in an increase in grain size and surface roughness.

3.2. Optical and electronic properties

In Fig. 4a and b, plots of the electrical resistivity measured as a function of temperature are shown for V_2O_3 films on C and A-sapphire substrates. The metal-insulator transition occurs at a temperature of about 150 K in both films. Fig. 4c shows the metal-insulator transition for a single crystal of $V_{2-y}O_3$, with $y=0.000$, grown and annealed at Purdue University. The transition is slightly broadened in the films compared with the single crystal, and displays a temperature hysteresis of about 20 K. Transition broadening has been seen for other V_2O_3 films [9–16], and attributed to the strain induced by lattice mismatch. The change in resistivity at the transition temperature is about eight orders of magnitude for the single crystal, while it is about
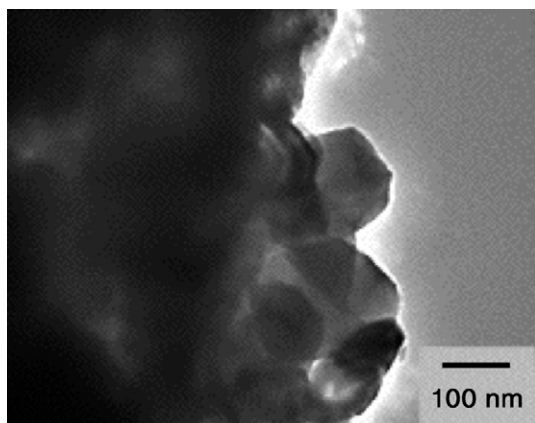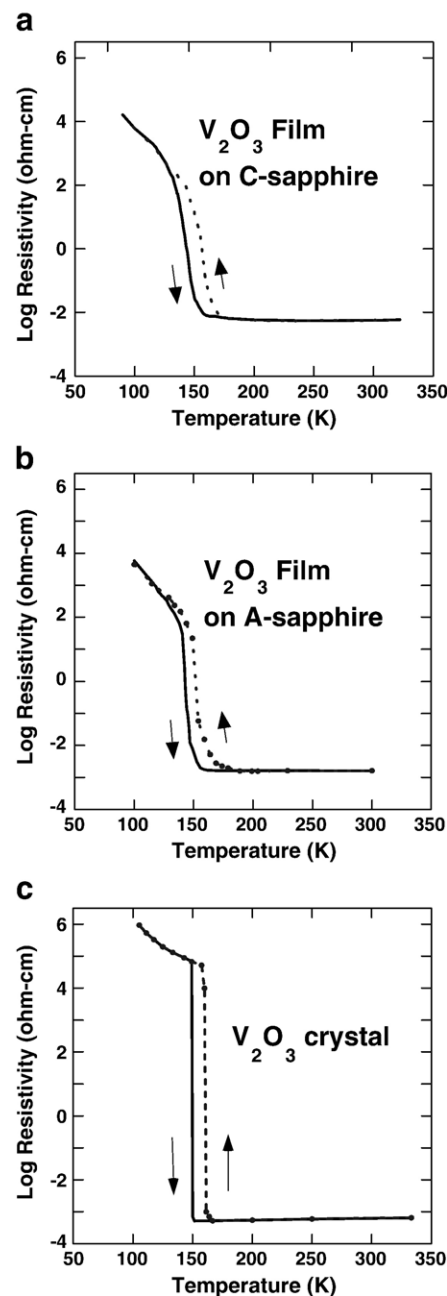
Fig. 4. Electrical resistivity versus temperature for (a) 300 nm thick V_2O_3 film on oriented C-plane sapphire substrate, (b) 300 nm thick V_2O_3 film on oriented A-plane sapphire substrate, and (c) single crystal V_2O_3.

six in the films. These measurements suggest that the films are stoichiometric and that the electrical properties of the films do not differ greatly from those of the bulk material.

The optical transmittance of a V_2O_3 film on C-sapphire and A-sapphire recorded at temperatures above and below the phase transition in presented in Fig. 5. The figure shows the switching of the optical transmission from about 40% at 5 µm near room temperature to about 80% at 77 K. This is consistent with the existence of an electrical transition in the V_2O_3 films from a metal at room temperature, to an insulator below the 150 K transition. The value of the room temperature transmission is dependent upon the thickness of the film.

Fig. 3. Bright-field TEM image of crystallites from a V_2O_3 film removed from the substrate.
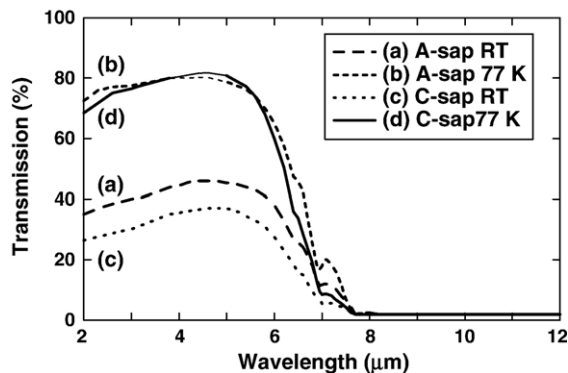
Fig. 5. Optical transmission at room temperature and 77 K for 500 nm thick V_2O_3 films deposited on C and A oriented sapphire substrates.

The electrical conductivity versus temperature for several $(V_{1-x}Cr_x)_2O_3$ films is given in Fig. 6a. Presented for reference, Fig. 6b is a plot, extracted from Ref. [6], depicting the changes in the electrical conductivity of chromium doped V_2O_3 crystals as a function of temperature. It can be seen that the metal-

Fig. 7. Optical transmission versus temperature of $(V_{1-x}Cr_x)_2O_3$ films deposited on (0 0 0 1) sapphire for varying chromium concentration.

insulator phase transition is present in chromium doped V_2O_3 films, and that their electrical properties do not differ greatly from those found in single crystals. As in the un-doped films, the transitions are somewhat broader and the magnitude of the transitions is less than is seen in the single crystal samples.

The optical transmittance of $(V_{1-x}Cr_x)_2O_3$ films on C-sapphire as a function of temperature is presented in Fig. 7. The un-doped film shows a transition at 150 K from a metal with a transmission of about 7% to an insulator with a transmission of about 60%. Referring to the single crystal behavior presented in Fig. 6b, the films show a similar behavior with an increase in the low temperature metal-insulator transition temperature with increasing chromium concentration. The higher temperature transition appears in the optical transmission measurement. It is also broadened and reduced in magnitude relative to measurements on single crystals.

Fig. 8 is a plot of the optical transmission at 4 micron versus temperature for annealed, non-stoichimetric $V_{2-y}O_3$ films. As referenced in Fig. 1, the metal-insulator transition temperature decreases with increasing non-stoichiometry. The values for y
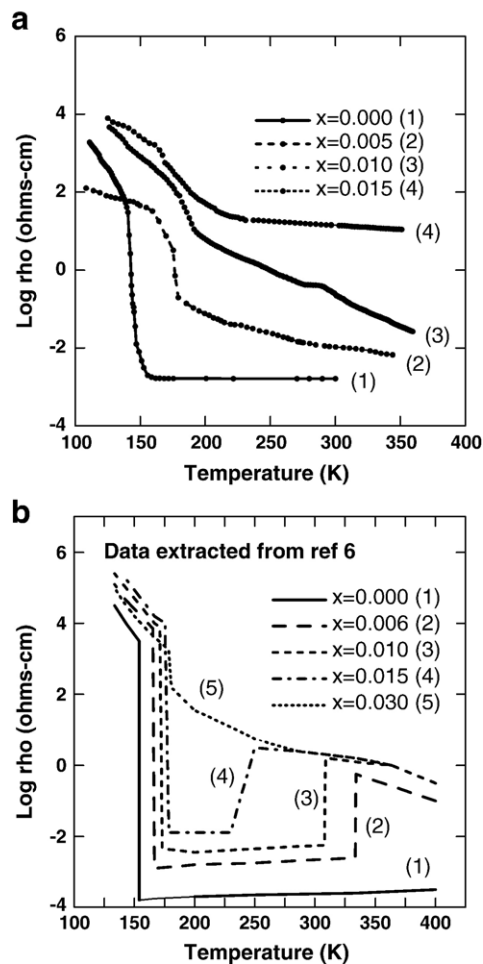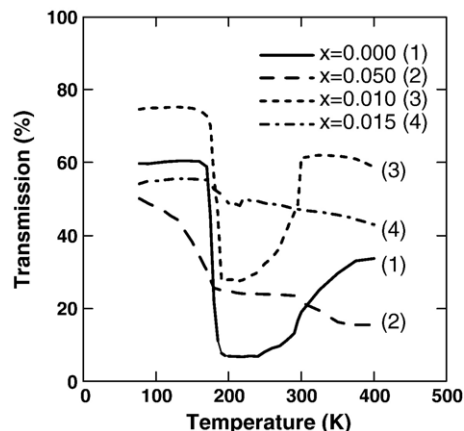

Fig. 6. Electrical resistivity versus temperature of $(V_{1-x}Cr_x)_2O_3$ for varying chromium concentration. (a) The electrical resistivity versus temperature for $(V_{1-x}Cr_x)_2O_3$, films on C oriented sapphire, data taken on cooling. (b) The electrical resistivity versus temperature for single crystal $(V_{1-x}Cr_x)_2O_3$, data taken on cooling (extracted from Ref. [6]).
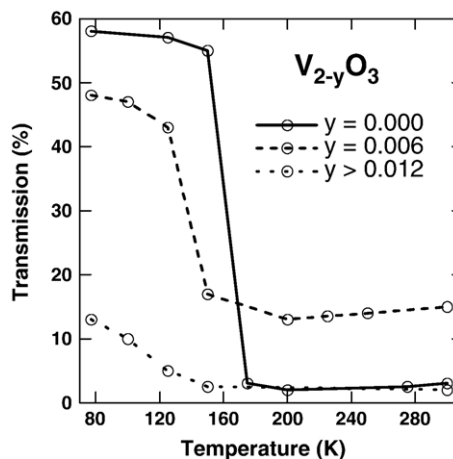
Fig. 8. The optical transmission versus temperature for $V_{2-y}O_3$ films deposited on (0 0 0 1) sapphire. The varying degrees of non-stoichiometry (y) obtained by annealing at low oxygen partial pressures in a controlled atmosphere, vertical quench furnace.

given in Fig. 8 have been extrapolated from transition temperatures for the data on single crystals from Ref. [7]. The transitions are again very broad and decreased in amplitude. In addition, it was found that to obtain the same transition temperature and degree of non-stoichiometry, the films must be annealed at much lower oxygen pressures than for the single crystals. It is possible that a small amount of re-oxidation occurs during the quench, which is insignificant in the bulk crystals, but is significant for the small grains in the films. From Fig. 1, it can be seen that below $y = 0.012$, the transitions occur below the 77 K temperature limit of the optical measurements.

4. Conclusions

Films with thicknesses from 125 nm to 1250 nm of V_2O_3 and chromium doped V_2O_3 films on sapphire substrates have been grown using the sol–gel method. The un-doped films were subsequently annealed under controlled oxygen atmospheres. Examination by XRD, SEM, TEM and AFM revealed that the films were comprised of well-formed, highly oriented grains. Optical transmission and resistivity measurements revealed that the films undergo phase transitions similar to those of single crystals. In comparison with the known phase diagram for the single crystal $V_{2-y}O_3$ and $(V_{1-x}Cr_x)_2O_3$ system, it can be seen that the films exhibit a similar phase relationship. The PM to AFI transition temperature decreases from about 150 K as the vanadium to oxygen ratio is changed by annealing. The PM to AFI transition increases as the chromium concentration is increased and a higher temperature PM to PI transition appears.

References

[1] D. McWhan, T. Rice, J. Remeika, Phys. Rev. Lett. 23 (1969) 1384.
[2] D. McWhan, J. Remeika, Phys. Rev., B 2 (1970) 3734.
[3] M. Nakahira, S. Horichi, H. Ooshima, J. Appl. Phys. 41 (1970) 836.
[4] D. McWhan, J. Remeika, T. Rice, W. Brinkman, W. Maita, A. Menth, Phys. Rev. Lett. 27 (1971) 941.
[5] D. McWhan, A. Menth, J. Remeika, W. Brinkman, T. Rice, Phys. Rev., B 7 (1973) 1920.
[6] H. Kuwamoto, J. Honig, J. Appel, Phys. Rev., B 22 (1980) 2626.
[7] S. Shivashankar, J. Honig, Phys. Rev., B 28 (1983) 5695.
[8] F. Chudnovski, V. Andreev, V. Kuksenko, V. Piculin, D. Frolov, P. Metcalf, J. Honig, J. Solid State Chem. 133 (1997) 430.
[9] F. Case, J. Vac. Sci. Technol., A 9 (1991) 461.
[10] K. Rogers, J. Coath, M. Lovell, J. Appl. Phys. 70 (1991) 1412.
[11] D. Partow, S. Gurkovich, K. Radford, L. Denes, J. Appl. Phys. 70 (1991) 443.
[12] H. Schuler, S. Klimm, G. Weissmann, C. Renner, S. Horn, Thin Solid Films 299 (1997) 119.
[13] I. Yamaguchi, T. Manabe, T. Kumagai, W. Kondo, S. Mizuta, Thin Solid Films 366 (2000) 294.
[14] P. Jin, M. Tazawa, K. Yoshimura, K. Igurashi, S. Tanemura, K. Macak, U. Helmersonn, Thin Solid Films 375 (2000) 128.
[15] B. Sass, C. Tusche, W. Felsch, N. Quaas, A. Weismann, M. Wenderoth, J. Phys., Condens. Matter 16 (2004) 77.
[16] C. Muller, A.A. Nateprov, G. Obermeier, M. Klemm, R. Tidecks, A. Wixforth, S. Horn, J. Appl. Phys. 98 (2005) 84111.
[17] Q. Guo, D. Kim, S. Street, D. Goodman, J. Vac. Sci. Technol., A 17 (1991) 1887.
[18] J. Biener, M. Baumer, R. Madix, P. Liu, E. Nelson, T. Kendelewicz, G. Brown, Surf. Sci. 441 (1999) 1.
[19] H. Miyazaki, M. Kamei, I. Yasui, Thin Solid Films 343–344 (1999) 168.
[20] Q. Guo, S. Lee, D. Goodman, Surf. Sci. 437 (1999) 38.
[21] P. Jin, M. Tazawa, M. Ikeyana, S. Tanemura, K. Macak, X. Wang, S. Olafsson, U. Hellmersonn, J. Vac. Sci. Technol., A 17 (1999) 1817.
[22] A. Dupuis, M. Haija, B. Richter, H. Kuhlenbeck, H. Freund, Surf. Sci. 539 (2003) 99.
[23] Q. Luo, Q. Guo, E.G. Wang, Appl. Phys. Lett. 84 (2004) 2337.
[24] S. Yonezawa, Y. Muraoka, Y. Ueda, Z. Hiroi, Solid State Commun. 129 (2004) 245.
[25] J. Schoiswohl, M. Sock, S. Surnev, M. Ramsey, F. Netzer, G. Kresse, J. Anderson, Surf. Sci. 555 (2004) 101.
[26] B. Sass, C. Tusche, W. Felsch, F. Bertran, F. Fortuna, P. Ohresser, G. Krill, Phys. Rev., B 71 (2005) 014415.
[27] F. Pfuner, J. Schoiswohl, M. Sock, S. Surnev, M. Ramsey, F. Netzer, J. Phys., Condens. Matter 17 (2005) 4035.
[28] C. Greenberg, D. Singleton, Sol. Energy Mater. 16 (1987) 501.
[29] J. Piao, S. Takahasi, S. Kohiki, Jpn. J. Appl. Phys. 37 (1998) 6519.
[30] J. Shepherd, C. Sandberg, Rev. Sci. Instrum. 55 (1984) 1696.